THE JOURNAL OF PHYSICAL CHEMISTRY C

Article

Cite This: J. Phys. Chem. C 2018, 122, 24658−24664

pubs.acs.org/JPCC

Potential Routes and Mitigation Strategies for Contamination in Interfacial Specific Infrared Spectroelectrochemical Studies

Marco Dunwell, Xuan Yang, Yushan Yan,* and Bingjun Xu*

Center for Catalytic Science and Technology, Department of Chemical and Biomolecular Engineering, University of Delaware, Newark, Delaware 19716, United States

Supporting Information

ABSTRACT: Attenuated total reflectance surface-enhanced infrared absorption spectroscopy (ATR-SEIRAS) is a powerful tool for probing the electrochemical interface; however, inconsistencies in reported spectroscopic observations persist. In this work, we identify potential sources of contamination in ATR-SEIRAS using CO as a probe molecule by varying the electrolyte purity, counter electrode (CE), and anolyte/catholyte separator. We show that only a linearly bound CO near 2050−2100 cm^{-1} is observed in clean experiments, whereas the use of low-purity electrolytes and Pt CEs leads to additional bands near 1800−1950 and 1920−2020 cm^{-1}, respectively, which are commonly assigned to bridge-bonded CO in the previous literature. These observations highlight the extreme sensitivity of ATR-SEIRAS and the importance of avoiding contaminants which lead to additional spectroscopic features.

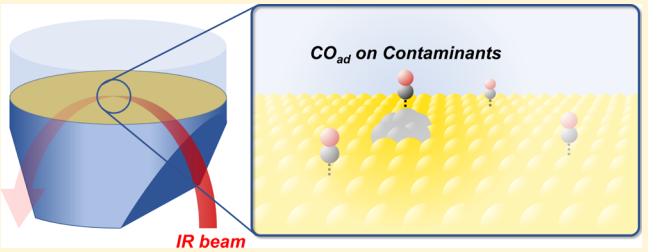

INTRODUCTION

The development of in situ and operando interfacial specific infrared spectroscopic techniques such as polarization-modulated infrared reflection absorption spectroscopy (PM-IRRAS) and attenuated total reflectance surface-enhanced infrared absorption spectroscopy (ATR-SEIRAS) represents a significant step forward in probing surface-mediated electrochemical processes.[4−9] With the rise in popularity of coupled infrared spectroscopic and electrochemical studies, however, inconsistencies in reported spectroscopic observations have arisen. A notable example is CO adsorption on Au electrodes observed during various investigations of small-molecule oxidation (such as CO, formate, or methanol) or reduction (such as CO_2).[1−3,10−20]

Four primary vibrational modes have been assigned to CO adsorbed on Au electrodes during spectroelectrochemical studies (Table 1), attributed to linearly bound CO (CO_L),[1−3,10−21] bridge-bound CO (CO_B),[1−3,10−13,17−20] multibound CO (CO_M),[2,17] and weak linearly bound CO (CO_{WL}).[12,13] The appearance of each of these bands, however, is not consistent throughout the literature, even under similar experimental conditions. For example, CO_{WL} is only observed by Chen et al., both in acidic and in alkaline electrolytes.[12,13] CO_M is observed by Blizanac et al. at 1981 cm^{-1} on Au(110), whereas Chang et al. report only a single CO_L band centered at ∼2100 cm^{-1} on the same facet.[2,11] Similarly, on Au(111) facets Blizanac et al. observe no CO_L band, but do observe a pronounced CO_B band at 2042 cm^{-1} in 0.1 M $HClO_4$, whereas Rodriguez et al. report two bands at 2000 and ∼1910 cm^{-1} assigned to CO_L and CO_B, respectively, in 0.1 M NaOH.[2,17,18] The discrepancy in wavenumber can be explained by the difference in potential between the two experiments because of the Stark tuning effect;[22] however, the appearance of the CO_L band only in NaOH is unexpected, particularly as the intensity of the CO_L band is expected to decrease at lower standard hydrogen electrode potentials.[14,20,23] The primary inconsistency between experiments is related to the observation of the CO_B band among polycrystalline Au electrodes (Au_{PC}). Several reports observe only a single, higher-wavenumber band attributed to CO_L,[14−16,19,21] whereas others report two bands, with the higher- and lower-wavenumber bands assigned to CO_L and CO_B, respectively.[1,12,13,19,20] Moreover, conflicting reports of either a lone CO_L band or both CO_L and CO_B bands can be found in acidic,[1,12,13,15,16,19] neutral,[14,20] and alkaline[13,15,21] electrolytes, so that these discrepancies cannot be simply attributed to differences in the electrolyte or potential range studied. Finally, Sun et al. report two separate bands related to CO_L.[19] One band from 2110 to 2136 cm^{-1} resembles features observed in other studies, whereas a lower band from 2020 to 2045 cm^{-1} falls between the typical CO_L and CO_B bands commonly observed on Au_{PC}. This lower-wavenumber band was attributed to CO_L adsorbed more strongly to specific sites of the electrode such as grain boundaries or very near the Si substrate on which the Au_{PC} film is deposited.[16] Despite these numerous examples, the origin of the inconsistencies in the existing literature remains poorly understood.

Received: June 13, 2018
Revised: September 22, 2018
Published: October 9, 2018

DOI: 10.1021/acs.jpcc.8b05634
J. Phys. Chem. C 2018, 122, 24658−24664

Table 1. Reported CO Adsorption Band Assignments and Peak Positions in cm^{-1}

author	electrode	CE[a]	electrolyte	CO_L[b]	CO_{WL}[c]	CO_B[d]	CO_M[e]
Beden[1]	Au	N/A	$HClO_4$	2080		1940	
Blizanac[2,3]	Au(111)	N/A	$HClO_4$			2042	1954
	Au(100)	N/A	$HClO_4$			2017	
	Au(110)	N/A	$HClO_4$	2124		2021	1981
Chang[11]	Au(210)	N/A	$HClO_4$	2100−2115		1930−1985	
	Au(210)	N/A	KOH			1920−1990	
Chang[10]	Au(210)	Au	$HClO_4$	2105−2115			
	Au(110)	Au	$HClO_4$	2090−2110			
Chen[12]	Au	Pt	$HClO_4$	2036	2110	1846	
Chen[13]	Au	Pt	NaOH	2000	2100	1930	
Corrigan[21]	Au	N/A	NaOH	1940			
Dunwell[14]	Au	graphite	$NaHCO_3$	2050−2100			
Kunimatsu[15]	Au	Au	NaOH	1940−2000			
	Au	Au	$HClO_4$	1990−2050			
Miyake[16]	Au	Au	$HClO_4$	2108			
Rodriguez[17]	Au(111)	Au	NaOH	2000		1900	1830
Rodriguez[18]	Au(111)	Au	NaOH + MeOH	2000		1920	
Sun[19]	Au	N/A	$HClO_4$	2110−2136			
				2020−2045			
	Au (flame annealed)	N/A	$HClO_4$	2110−2136		1925−1975	
				2020−2045			
Wuttig[20]	Au	Pt	$NaHCO_3$	2110		1930−2030	
this work[f]	Au	graphite	$NaHCO_3$	2075−2104			

[a]N/A indicates that the type of CE used was not indicated in the cited work. [b]CO_L: linearly or atop-bound CO. [c]CO_{WL}: weakly bound linear or atop CO. [d]CO_B: bridge-bound CO. [e]CO_M: multibound or CO adsorbed on hollow sites. [f]Results when using the standard conditions as defined by experiment 1 in Table 2.

In this work, we demonstrate two modes of working electrode (WE) contamination as possible sources of the differences in CO adsorption on Au electrodes and discuss mitigation strategies. We show that the lower-wavenumber band commonly associated with CO_B is likely caused by electrolyte impurities by monitoring CO adsorption using ATR-SEIRAS in three electrolytes of different purities: high-purity sodium bicarbonate, which is further purified via chelation; the same high-purity electrolyte without additional purification; and finally using low-purity sodium bicarbonate. Additionally, we show that the use of Pt counter electrodes (CEs) causes the appearance of an additional band associated with CO_L on Pt, which was previously assigned to CO_B on Au. Although all studies presented in this work were conducted with an Au film WE in near-neutral pH electrolytes, the general sources of contamination (the electrolyte and CE) as well as the proposed mitigation strategies should be independent of both WE structure and composition. The contamination, however, may manifest differently on different electrodes or with different electrolytes, as the wavenumber and intensity of vibration bands originating from the contaminant and adsorbates on the WE may vary, and contaminants may deposit at different rates or potentials on different materials or at different pH.[24] Avoiding these common routes of contamination in spectroelectrochemical studies is key to developing a proper and widely accepted understanding of adsorbate behavior during electrochemical processes.

METHODS AND MATERIALS

Materials. Au film electrodes for ATR-SEIRAS measurements were prepared via a chemical deposition method detailed in our previous work.[14,16] Graphite rod CEs (99.995%, Aldrich) were sonicated in deionized-distilled water (Banstead Mega-Pure Water Purification System) to remove all loose graphite prior to use. Pt wire CEs (99.95%, Alfa Aesar) were cleaned by immersing in a 3:1 by volume solution of H_2SO_4 (95−98%, Sigma-Aldrich) and H_2O_2 (30%, Sigma-Aldrich) and rinsing in deionized-distilled water prior to each use. Experiments were conducted in 0.5 M $NaHCO_3$ solutions of various purities. Low-purity electrolytes were prepared using $NaHCO_3$ (99.7%, Sigma-Aldrich). Moderate-purity 0.5 M $NaHCO_3$ electrolytes were prepared by purging 0.25 M Na_2CO_3 (99.999%, EMD Millipore) overnight with high-purity CO_2 gas. For the highest purity experiments, these electrolytes were further purified by stirring overnight after the addition of 5 g of a solid-supported iminodiacetate resin (Chelex 100, Sigma-Aldrich) for every 100 mL of electrolyte.[25] Electrolytes were purged with CO gas (Matheson) for >15 min prior to each experiment (solution pH = 8.7) to saturate the solution with CO and remove the remaining CO_2. All experiments were conducted under continuous CO purge.

ATR-SEIRAS Measurements. All ATR-SEIRAS measurements were collected in a three-electrode electrochemical cell with a chemically deposited polycrystalline Au film as the WE, a graphite rod or Pt wire as the CE, and an Ag/AgCl (3.0 M KCl, BASi) reference electrode (RE) described in our previous work.[26] The REs and CEs were separated by a proton exchange membrane (Nafion 211, Fuel Cell Store) unless otherwise noted. All presented spectra are eight co-added scans with 4 cm^{-1} resolution and potentials are given on the reversible hydrogen electrode (RHE) scale unless otherwise noted. All potentials given were actively corrected for internal resistance of the spectroelectrochemical cell following impedance measurement. Spectra were collected using an Agilent CARY 660 FTIR spectrometer outfitted with a custom spectroelectrochemical cell detailed in our previous work.

DOI: 10.1021/acs.jpcc.8b05634
J. Phys. Chem. C 2018, 122, 24658−24664

Electrochemical measurements were conducted with a Solartron 1287/1260 potentiostat.

Metal contamination experiments were conducted by first activating the Au film for SEIRAS measurements in 0.5 M $NaHCO_3$ under continuous CO purge by stepping the potential from 1.0 to 0.0 to −0.4 V. The potential was held at 0.0 and −0.4 V for less than 30 s at each potential to minimize electrodeposition of impurities prior to collection of the SEIRA spectra. After activation, the background was collected (128 co-added scans) at 1.0 V so that no adsorbed CO is present in the background. The initial set of spectra (0 min) was then collected continuously during cyclic voltammetry (CV) from −0.7 to 1.0 V with a scan rate of 10 mV s^{-1}. After a single cycle, the potential was held at −0.7 V for 15 min to allow for deposition of metal ion impurities on the Au film electrode. After 15 min, a second set of spectra was collected using the same CV procedure detailed above. Additional sets of spectra were then collected during CV after 30, 45, and 60 min time points at −0.7 V. Following the final spectroscopic measurements, the electrolyte was saturated with Ar for >15 min and CVs were collected at 50 mV s^{-1} from 0.0 to 1.2 V.

RESULTS AND DISCUSSION

Sources of contamination of Au films during ATR-SERIAS experiments were investigated on Au film electrodes by conducting a series of experiments in which the electrolyte purity, the CE, and the membrane separator between the WEs and CEs were varied (Table 2). The standard experiment was conducted using high-purity sodium bicarbonate, which was further purified using a chelating resin,[25] a graphite rod CE, and a Nafion separator between the anode and cathode compartments. A single band, assigned to linearly bound CO on Au, is observed from 2075 to 2104 cm^{-1} between 0 and 0.6 V (Figure 1a). Additionally, a minor band with intensities barely above the detection limit, probably because of CO adsorption on the metal impurity band, is observed near 1930 cm^{-1}. The same features, with nearly the same relative intensities, are observed after 15 (Figure S1b), 30 (Figure S1c), 45 (Figure S1d), and 60 min (Figure 1b) of electrolysis at −0.7 V, suggesting no significant change during potentiostatic measurement. The decrease in signal intensity with time is due to degradation of the metal film caused by the high current and accompanying bubble formation during the potential hold at −0.7 V. The consistency of the spectra over the course of the 1 h test suggests that the electrolyte is sufficiently pure to avoid significant metal impurity contamination of the Au film electrode.

Table 2. Variation of Key Experimental Parameters for Different Experiments To Test Sources of Contamination in ATR-SEIRAS Experiments

experiment	film	$NaHCO_3$ purity	membrane	CE
1	Au	99.999%, chelated	Nafion 211	graphite rod
2	Au	99.999%	Nafion 211	graphite rod
3	Au	99.7%	Nafion 211	graphite rod
4	Au	99.999%, chelated	Nafion 211	Pt wire
5	Au	99.999%, chelated	N/A	Pt wire

The effect of electrolyte purity was then examined by repeating the experiment in the same high-purity bicarbonate electrolyte (99.999%) without additional purification and again with a lower purity bicarbonate electrolyte (99.7%). The high-purity, nonchelated electrolyte yields similar spectral behavior to that of the standard experiment, suggesting that the as-purchased sodium carbonate salt is sufficiently pure for spectroscopic measurements (Figure S2). Conversely, when the experiment was repeated in the low-purity bicarbonate electrolyte, the minor peak observed in the standard sample at a lower wavenumber (~1930 cm^{-1}) grew significantly with time, reaching roughly the same intensity as the CO_{Au} band (Figures 1c,d and S3). This additional band, often assigned to bridge-bonded CO on Au in the literature, is observed from 1800 to 1975 cm^{-1} across the entire potential range examined (−0.7 to 1.0 V). The appearance of this band only in the impure electrolyte, however, suggests that it is not related to CO adsorption on a pristine Au surface. Additional spectral features because of electrolyte impurities could arise from two different sources: (1) surface reconstruction of the electrode because of strongly adsorbing impurities such as halides or (2) metal impurities which are electrodeposited onto the Au film electrode at low potentials. The first possibility is unlikely, however, as the impurity band grows after holding at −0.7 V, where halides will be electrostatically repelled from the electrode, and diminishes significantly after the potential is swept to 1.0 V, so that it is nearly absent during the cathodic sweep (Figures 2a,b and S4). The second possibility is more consistent with spectroscopic observation, as the lower-wavenumber band increases after holding at low potential where metal ion contaminants will be electrodeposited onto the Au film and decreases at high potentials where metal contamination can be oxidized from the electrode. The hysteresis between anodic and cathodic sweeps can also be explained by the time necessary for metal ions to be reduced once again onto the surface. It should be noted that this metal contamination band is similar to features commonly assigned to bridge-bonded CO on Au in a number of previous works, suggesting that metal ion impurities are probably the cause of misinterpretation of data in the existing PM-IRRAS and ATR-SEIRAS literature.[12,13,19] Chen et al. reported growth of bands at 1846 and 1900−1950 cm^{-1} during potentiostatic measurements at −0.2 V versus Ag/AgCl in 0.1 M $HClO_4$ and from 0.05 to ~1.0 V versus Ag/AgCl in 0.1 M NaOH, respectively.[12] Moreover, the bands in NaOH exhibit the same hysteresis observed in this work, with the lower-wavenumber band only appearing during the anodic sweep following a potential hold at 0.0 V versus Ag/AgCl. On the basis of these similarities, it is likely that these bands, originally attributed to CO_B on Au, are due to CO adsorption on metal impurities in the electrolyte. We chose not to speculate on the specific identity of the metal impurities in this work, as a comprehensive list of possible impurities is not enumerated in the specification sheets provided and identification of these species because of the location of the adsorbed CO band is not definitive because of the coverage dependence of band position and the similarity of the band position with a wide variety of metal contaminants.[27,28] Future studies using X-ray photoelectron spectroscopy or inductively coupled plasma mass spectrometry, however, may be able to definitively identify the metal contaminants. Because of the extreme sensitivity of SEIRAS,[8,29] high-purity electrolytes or, in the case of lower-purity electrolytes, additional electrolyte purification steps, such as chelation or pre-electrolysis to electrodeposit metal contaminants on a sacrificial metal electrode are necessary to obtain clean spectroscopic measurements.

DOI: 10.1021/acs.jpcc.8b05634
J. Phys. Chem. C 2018, 122, 24658−24664

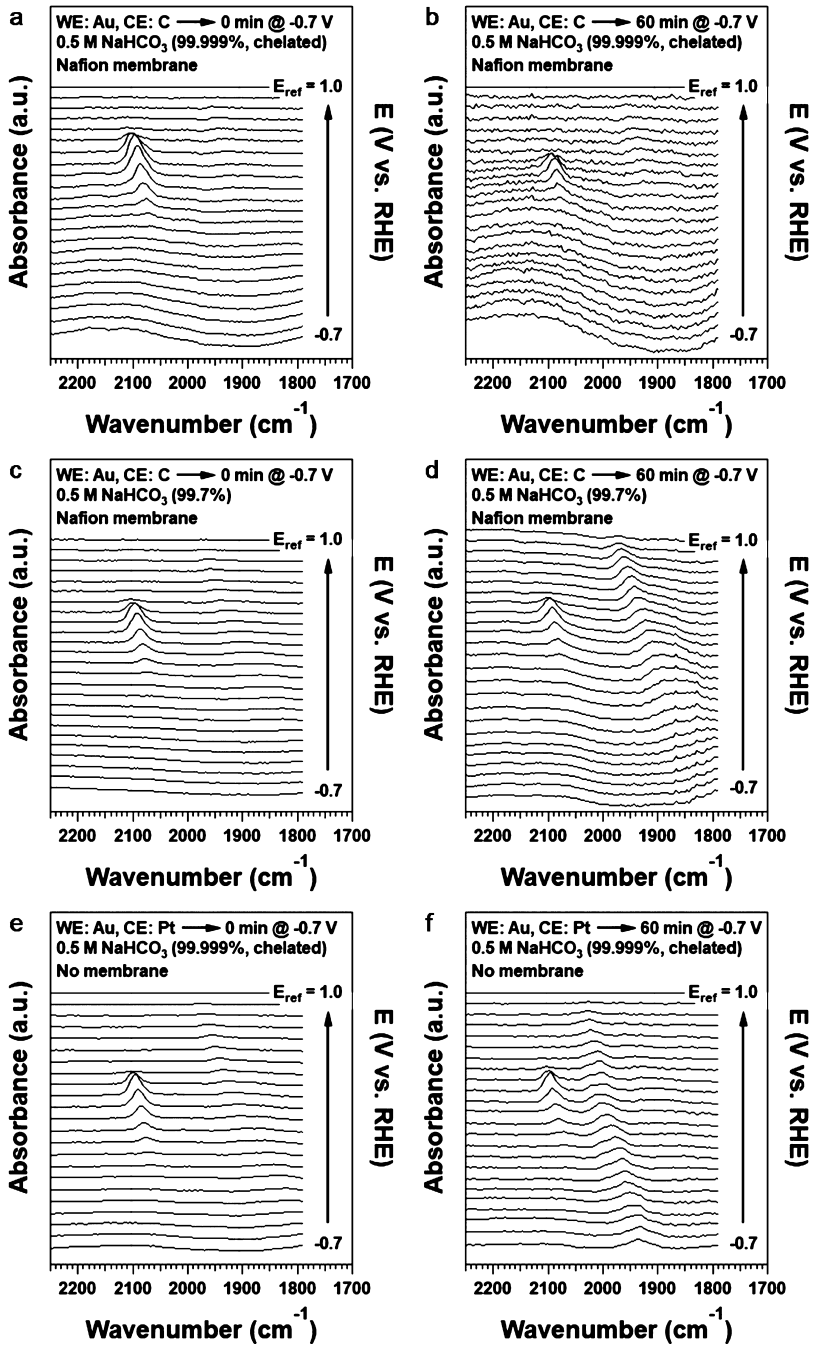

Figure 1. ATR-SEIRA spectra collected during an anodic potential sweep from −0.7 to 1.0 V at 10 mV s^{-1} (a) prior to and (b) after 60 min at −0.7 V in chelated, high-purity 0.5 M $NaHCO_3$ with a graphite CE and Nafion separator, (c) prior to and (d) after 60 min at −0.7 V in low-purity 0.5 M $NaHCO_3$ with a graphite CE and Nafion separator, and (e) prior to and (f) after 60 min at −0.7 V in chelated, high-purity 0.5 M $NaHCO_3$ with a Pt CE and no separator between the anolyte and catholyte. All spectra were collected with 4 cm^{-1} resolution and eight co-added scans and are presented using a reference spectrum at 1.0 V under continuous CO purge.

In addition to metal ion impurities from the electrolyte, contamination from the use of a Pt CE was studied by repeating the standard experiment, replacing the graphite rod CE with a Pt wire, with and without a Nafion membrane separating the WE and CE chambers. When a Nafion membrane is used, the spectra show no significant deviation from the standard case, suggesting that the membrane effectively blocks Pt crossover (Figure S5). In the absence of the membrane, however, an additional band appears from 1930 to 2030 cm^{-1}, which is present at all potentials below 1.0 V (Figures 1e,f and S6). The band position is consistent with linearly bound CO on Pt at low coverage,[27,28,30] indicating contamination from the Pt CE. Moreover, this band does not show significant hysteresis between the anodic and cathodic sweeps, suggesting that the adsorption site is not removed at high potential, which is again consistent with Pt, which does not form soluble oxides below 1.0 V (Figure 2c,d).[31] Together, these results strongly suggest that Pt contamination occurs through oxidation of the Pt wire CE, forming Pt ions which are subsequently electrodeposited on the Au WE. Indeed, an identical feature is observed in a previous study of the electroreduction of CO_2 on Au in which a Pt CE was used.[20]

DOI: 10.1021/acs.jpcc.8b05634
J. Phys. Chem. C 2018, 122, 24658−24664

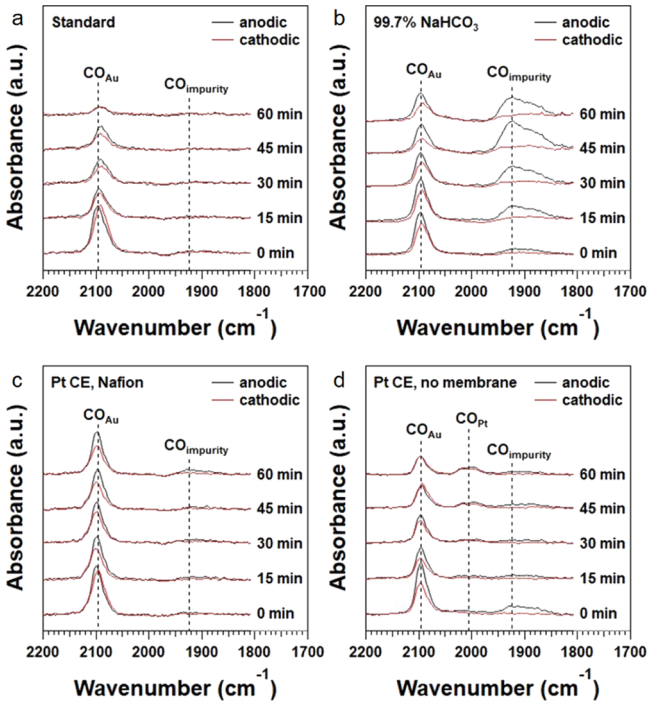

Figure 2. Time-dependent ATR-SEIRA spectra collected at 0.4 V during the anodic (black) and cathodic (red) branches of CVs from −0.7 to 1.0 V at 10 mV s^{-1} (a) under standard conditions, (b) using low-purity 0.5 M $NaHCO_3$, (c) using a Pt CE with a Nafion separator, and (d) using a Pt CE with no separator between the anolyte and catholyte. All spectra were collected with 4 cm^{-1} resolution and eight co-added scans and are presented using a reference spectrum at 1.0 V.

Note that although trace Cl^- concentration from the Ag/AgCl RE used in this work may promote Pt dissolution, no additional contaminants on the WE are expected with graphite as the CE. This band was previously attributed to irreversibly adsorbed bridge-bonded CO on Au, suggesting significant CO coverage under CO_2 reduction conditions, contrary to subsequent findings.[14,20] The misattribution of CO on Pt contaminants could lead to significant differences in mechanistic understanding, as rate expressions and therefore expected Tafel slope values depend on the surface coverage of various adsorbates. In order to avoid Pt contamination in future studies, researchers should use graphite or metal CEs of the same composition as the WE. If an experiment necessitates the use of a Pt CE, however, a Nafion membrane could be used to minimize the contamination from the CE.

Despite conspicuous changes in the spectra, cyclic voltammograms collected under Ar at the end of each experiment show no significant deviation from the standard sample (Figure 3). Each CV shows a broad wave at ∼0.8 V, previously assigned to either reconstruction of the Au surface on preferentially Au(111)-oriented electrodes[32,33] or to pseudocapacitance because of anion adsorption on the electrode surface.[33,34] It should be noted, however, that all CVs exhibit a small cathodic current below 0.5 V versus RHE that is atypical of clean, polycrystalline Au electrodes. This feature, however, is common in SEIRAS studies and is probably due to partial reduction of SiO_2 on the Si substrate.[35] In particular, no discernible peaks associated with Pt or other metal oxidation is observed.[36] When a Pt CE was used with no membrane, however, an increase in cathodic current is observed below 0.4 V, consistent with increased activity for

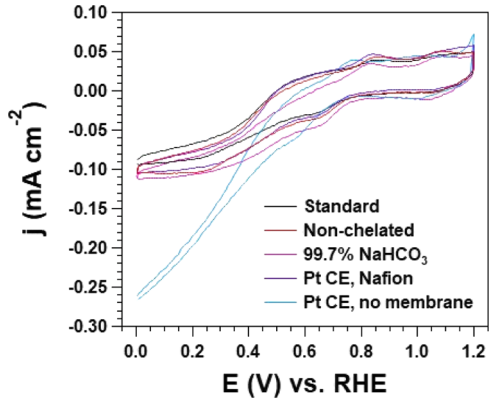

Figure 3. Steady-state cyclic voltammograms collected at 50 mV s^{-1} under Ar after each experiment given in Table 2.

early-onset hydrogen evolution because of Pt contamination (Figure 3).[37] It should be noted, however, that although a clear CO_{Pt} band is observed spectroscopically, the CV is free from both typical Pt-oxidation and reduction features and the characteristic hydrogen underpotential deposition peaks.[36] The lack of signature Pt features in the final CV indicates that the Pt coverage is sufficiently low that the current associated with Pt oxidation/reduction and hydrogen adsorption/desorption is negligible compared with the double-layer current observed on the base Au film. Thus, lack of the Pt feature in CV cannot be used as evidence to demonstrate the surface is free of Pt contamination.

On the basis of the observations from the spectra (summarized in Figure 4), we propose that only a single band from the CO stretch of CO_L should be observed on clean, polycrystalline Au electrodes. Note that any additional bands associated with additional organic products are not observed (Figure S7). These results, however, cannot be

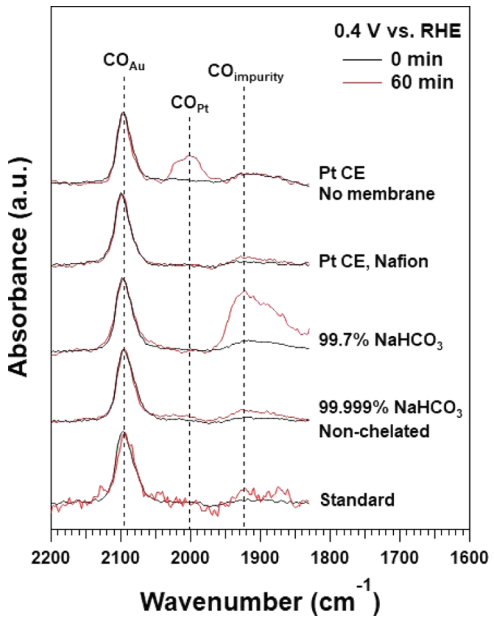

Figure 4. Summary of ATR-SEIRA spectra collected at 0.4 V during the anodic potential sweep prior to and after 60 min at −0.7 V under continuous CO purge under each experimental condition given in Table 1. All spectra were collected with 4 cm^{-1} resolution and eight co-added scans and are presented using a reference spectrum at 1.0 V.

DOI: 10.1021/acs.jpcc.8b05634
J. Phys. Chem. C 2018, 122, 24658−24664

directly applied to additional bands attributed to CO_B and CO_M which appear on clean single-crystal surfaces, so that discrepancies in these features are still not well-understood.[2,3,10,11,17,18] Importantly, the demonstration of additional spectroscopic features because of contamination under common experimental conditions underscores the importance of the use of extremely pure electrolytes and graphite CEs not only for CO adsorption on Au, but for all spectroelectrochemical studies. Investigations of electrochemical processes in which adsorbates and intermediates are relatively weakly bound, such as CO_2 and CO reduction on Ag and Cu electrodes,[38−42] are particularly susceptible to metal contamination, as features of interest can be easily drowned out by adsorption on more strongly binding metal contaminants. Elimination of metal contamination is imperative in obtaining an accurate understanding of the electrochemical interface via in situ and operando spectroelectrochemical studies.

CONCLUSIONS

Careful investigations of different modes of contamination of Au electrodes during ATR-SEIRAS measurements suggest that CO adsorption on Pt or other metal contaminants are the likely cause of discrepancies in CO adsorption behavior in the literature. We demonstrate that the use of insufficiently pure electrolytes and Pt CEs, particularly without a membrane separator, results in adsorbed CO bands distinct from those observed on clean polycrystalline Au electrodes. The contaminants lead to misinterpretation of adsorption behavior and potentially influence the development of reaction mechanisms based on the coverage of various species under reaction conditions. As a result, it is imperative that all future spectroelectrochemical studies are conducted in the highest available purity electrolytes, with additional purification via chelation or pre-electrolysis in cases where commercial electrolytes are insufficiently pure, with either graphite or metal CEs matching that of the WE.

ASSOCIATED CONTENT

Supporting Information

The Supporting Information is available free of charge on the ACS Publications website at DOI: 10.1021/acs.jpcc.8b05634.

ATR-SEIRA spectra collected under various conditions (PDF)

AUTHOR INFORMATION

Corresponding Authors

*E-mail: yanys@udel.edu (Y.Y.).
*E-mail: bxu@udel.edu (B.X.).

ORCID

Xuan Yang: 0000-0001-8750-0742
Yushan Yan: 0000-0001-6616-4575
Bingjun Xu: 0000-0002-2303-257X

Author Contributions

Experiments were performed by M.D. The article was written through contributions of all the authors. All the authors have given approval to the final version of the article.

Notes

The authors declare no competing financial interest.

ACKNOWLEDGMENTS

B.X. acknowledges the support of the National Science Foundation CAREER Program (award no. CBET-1744586). M.D. and Y.Y. acknowledge the support of the National Science Foundation—Chemical Catalysis Program (award no. CHE-1566138).

REFERENCES

(1) Beden, B.; Bewick, A.; Kunimatsu, K.; Lamy, C. Infrared Study of Adsorbed Species on Electrodes: Adsorption of Carbon Monoxide on Pt, Rh and Au. *J. Electroanal. Chem. Interfacial Electrochem.* **1982**, *142*, 345−356.

(2) Blizanac, B. B.; Arenz, M.; Ross, P. N.; Marković, N. M. Surface Electrochemistry of Co on Reconstructed Gold Single Crystal Surfaces Studied by Infrared Reflection Absorption Spectroscopy and Rotating Disk Electrode. *J. Am. Chem. Soc.* **2004**, *126*, 10130−10141.

(3) Blizanac, B. B.; Lucas, C. A.; Gallagher, M. E.; Arenz, M.; Ross, P. N.; Marković, N. M. Anion Adsorption, CO Oxidation, and Oxygen Reduction Reaction on a Au(100) Surface: The pH Effect. *J. Phys. Chem. B* **2004**, *108*, 625−634.

(4) Li, J.; Zheng, B.; Zhang, Q.-W.; Liu, Y.; Shi, C.-F.; Wang, F.-B.; Wang, K.; Xia, X.-H. Attenuated Total Reflection Surface-Enhanced Infrared Absorption Spectroscopy: A Powerful Technique for Bioanalysis. *J. Anal. Test.* **2017**, *1*, 8.

(5) Wain, A. J.; O'Connell, M. A. Advances in Surface-Enhanced Vibrational Spectroscopy at Electrochemical Interfaces. *Adv. Phys. X* **2017**, *2*, 188−209.

(6) Wang, H.; Zhou, Y.-W.; Cai, W.-B. Recent Applications of in Situ Atr-Ir Spectroscopy in Interfacial Electrochemistry. *Curr. Opin. in Electrochem.* **2017**, *1*, 73−79.

(7) Ye, J.-Y.; Jiang, Y.-X.; Sheng, T.; Sun, S.-G. In-Situ Ftir Spectroscopic Studies of Electrocatalytic Reactions and Processes. *Nano Energy* **2016**, *29*, 414−427.

(8) Osawa, M. Surface-Enhanced Infrared Absorption. In *Near-Field Optics and Surface Plasmon Polaritons*, Kawata, S., Ed.; Springer Berlin Heidelberg, 2001; Vol. *81*, pp 163−187.

(9) Osawa, M.; Ikeda, M. Surface-Enhanced Infrared Absorption of P-Nitrobenzoic Acid Deposited on Silver Island Films: Contributions of Electromagnetic and Chemical Mechanisms. *J. Phys. Chem.* **1991**, *95*, 9914−9919.

(10) Chang, S. C.; Hamelin, A.; Weaver, M. J. Dependence of the Electrooxidation Rates of Carbon Monoxide at Gold on the Surface Crystallographic Orientation: A Combined Kinetic-Surface Infrared Spectroscopic Study. *J. Phys. Chem.* **1991**, *95*, 5560−5567.

(11) Chang, S.-C.; Hamelin, A.; Weaver, M. J. Reactive and Inhibiting Adsorbates for the Catalytic Electrooxidation of Carbon Monoxide on Gold (210) as Characterized by Surface Infrared Spectroscopy. *Surf. Sci.* **1990**, *239*, L543−L547.

(12) Chen, D.-J.; Allison, T. C.; Tong, Y. Y. J. Mechanistic Insights into Electro-Oxidation of Solution Co on the Polycrystalline Gold Surface as Seen by in Situ Ir Spectroscopy. *J. Phys. Chem. C* **2016**, *120*, 16132−16139.

(13) Chen, D.-J.; Tong, Y. J. An in-Situ Electrochemical Ir Investigation of Solution Co Electro-Oxidation on a Polycrystalline Au Surface in an Alkaline Electrolyte: Identification of Active Reaction Intermediates. *J. Electroanal. Chem.* **2017**, *800*, 39.

(14) Dunwell, M.; Lu, Q.; Heyes, J. M.; Rosen, J.; Chen, J. G.; Yan, Y.; Jiao, F.; Xu, B. The Central Role of Bicarbonate in the Electrochemical Reduction of Carbon Dioxide on Gold. *J. Am. Chem. Soc.* **2017**, *139*, 3774−3783.

(15) Kunimatsu, K.; Aramata, A.; Nakajima, N.; Kita, H. Infrared Spectra of Carbon Monoxide Adsorbed on a Smooth Gold Electrode. *J. Electroanal. Chem. Interfacial Electrochem.* **1986**, *207*, 293−307.

(16) Miyake, H.; Ye, S.; Osawa, M. Electroless Deposition of Gold Thin Films on Silicon for Surface-Enhanced Infrared Spectroelectrochemistry. *Electrochem. Commun.* **2002**, *4*, 973−977.

DOI: 10.1021/acs.jpcc.8b05634
J. Phys. Chem. C 2018, 122, 24658−24664

(17) Rodriguez, P.; Garcia-Araez, N.; Koverga, A.; Frank, S.; Koper, M. T. M. Co Electroxidation on Gold in Alkaline Media: A Combined Electrochemical, Spectroscopic, and Dft Study. *Langmuir* **2010**, *26*, 12425−12432.
(18) Rodriguez, P.; Kwon, Y.; Koper, M. T. M. The Promoting Effect of Adsorbed Carbon Monoxide on the Oxidation of Alcohols on a Gold Catalyst. *Nat. Chem.* **2011**, *4*, 177−182.
(19) Sun, S.-G.; Cai, W.-B.; Wan, L.-J.; Osawa, M. Infrared Absorption Enhancement for Co Adsorbed on Au Films in Perchloric Acid Solutions and Effects of Surface Structure Studied by Cyclic Voltammetry, Scanning Tunneling Microscopy, and Surface-Enhanced Ir Spectroscopy. *J. Phys. Chem. B* **1999**, *103*, 2460−2466.
(20) Wuttig, A.; Yaguchi, M.; Motobayashi, K.; Osawa, M.; Surendranath, Y. Inhibited Proton Transfer Enhances Au-Catalyzed Co2-to-Fuels Selectivity. *Proc. Natl. Acad. Sci. U.S.A.* **2016**, *113*, E4585−E4593.
(21) Corrigan, D. S.; Gao, P.; Leung, L. W. H.; Weaver, M. J. Comparisons between Surface Infrared and Surface-Enhanced Raman Spectroscopies: Band Frequencies, Bandwidths, and Selection Rules for Pseudohalide and Related Adsorbates at Gold and Silver Electrodes. *Langmuir* **1986**, *2*, 744−752.
(22) Lambert, D. K. Vibrational Stark Effect of Adsorbates at Electrochemical Interfaces. *Electrochim. Acta* **1996**, *41*, 623−630.
(23) Dunwell, M.; Wang, J.; Yan, Y.; Xu, B. Surface Enhanced Spectroscopic Investigations of Adsorption of Cations on Electrochemical Interfaces. *Phys. Chem. Chem. Phys.* **2017**, *19*, 971−975.
(24) Kanani, N. *Electroplating: Basic Principles, Processes and Practice*; Elsevier, 2005; pp 1−353.
(25) Wuttig, A.; Surendranath, Y. Impurity Ion Complexation Enhances Carbon Dioxide Reduction Catalysis. *ACS Catal.* **2015**, *5*, 4479−4484.
(26) Dunwell, M.; Yang, X.; Setzler, B. P.; Anibal, J.; Yan, Y.; Xu, B. Examination of near-Electrode Concentration Gradients and Kinetic Impacts on the Electrochemical Reduction of Co2 Using Surface-Enhanced Infrared Spectroscopy. *ACS Catal.* **2018**, *8*, 3999−4008.
(27) Dunwell, M.; Yan, Y.; Xu, B. In Situ Infrared Spectroscopic Investigations of Pyridine-Mediated Co2 Reduction on Pt Electrocatalysts. *ACS Catal.* **2017**, *7*, 5410−5419.
(28) Yan; Li, Q.-X.; Huo, S.-J.; Ma, M.; Cai, W.-B.; Osawa, M. Ubiquitous Strategy for Probing ATR Surface-Enhanced Infrared Absorption at Platinum Group Metal−Electrolyte Interfaces. *J. Phys. Chem. B* **2005**, *109*, 7900−7906.
(29) Osawa, M., Surface-Enhanced Infrared Absorption Spectroscopy. In *Compendium of Surface and Interface Analysis*; The Surface Science Society of Japan, Ed.; Springer Singapore: Singapore, 2018; pp 697−706.
(30) Kunimatsu, K.; Sato, T.; Uchida, H.; Watanabe, M. Adsorption/Oxidation of CO on Highly Dispersed Pt Catalyst Studied by Combined Electrochemical and ATR-FTIRAS Methods: Oxidation of CO Adsorbed on Carbon-Supported Pt Catalyst and Unsupported Pt Black. *Langmuir* **2008**, *24*, 3590−3601.
(31) Pourbaix, M. J. N.; Van Muylder, J.; de Zoubov, N. Electrochemical Properties of the Platinum Metals. *Platinum Met. Rev.* **1959**, *3*, 47−53.
(32) Ataka, K.-i.; Osawa, M. In Situ Infrared Study of Water−Sulfate Coadsorption on Gold(111) in Sulfuric Acid Solutions. *Langmuir* **1998**, *14*, 951−959.
(33) Arihara, K.; Kitamura, F.; Ohsaka, T.; Tokuda, K. Characterization of the Adsorption State of Carbonate Ions at the Au(111) Electrode Surface Using in Situ Iras. *J. Electroanal. Chem.* **2001**, *510*, 128−135.
(34) Ataka, K.-i.; Yotsuyanagi, T.; Osawa, M. Potential-Dependent Reorientation of Water Molecules at an Electrode/Electrolyte Interface Studied by Surface-Enhanced Infrared Absorption Spectroscopy. *J. Phys. Chem.* **1996**, *100*, 10664−10672.
(35) Dunwell, M.; Yan, Y.; Xu, B. A Surface-Enhanced Infrared Absorption Spectroscopic Study of pH Dependent Water Adsorption on Au. *Surf. Sci.* **2016**, *650*, 51−56.
(36) Sheng, W.; Zhuang, Z.; Gao, M.; Zheng, J.; Chen, J. G.; Yan, Y. Correlating Hydrogen Oxidation and Evolution Activity on Platinum at Different Ph with Measured Hydrogen Binding Energy. *Nat. Commun.* **2015**, *6*, 5848.
(37) Strmcnik, D.; Li, D.; Lopes, P.; Tripkovic, D.; Kodama, K.; Stamenkovic, V.; Markovic, N. When Small Is Big: The Role of Impurities in Electrocatalysis. *Top. Catal.* **2015**, *58*, 1174−1180.
(38) Firet, N. J.; Smith, W. A. Probing the Reaction Mechanism of Co2 Electroreduction over Ag Films Via Operando Infrared Spectroscopy. *ACS Catal.* **2016**, *7*, 606−612.
(39) Gunathunge, C. M.; Li, X.; Li, J.; Hicks, R. P.; Ovalle, V. J.; Waegele, M. M. Spectroscopic Observation of Reversible Surface Reconstruction of Copper Electrodes under Co2 Reduction. *J. Phys. Chem. C* **2017**, *121*, 12337.
(40) Heyes, J.; Dunwell, M.; Xu, B. Co2 Reduction on Cu at Low Overpotentials with Surface-Enhanced in Situ Spectroscopy. *J. Phys. Chem. C* **2016**, *120*, 17334−17341.
(41) Wuttig, A.; Liu, C.; Peng, Q.; Yaguchi, M.; Hendon, C. H.; Motobayashi, K.; Ye, S.; Osawa, M.; Surendranath, Y. Tracking a Common Surface-Bound Intermediate During Co2-to-Fuels Catalysis. *ACS Cent. Sci.* **2016**, *2*, 522−528.
(42) Pérez-Gallent, E.; Figueiredo, M. C.; Calle-Vallejo, F.; Koper, M. T. M. Spectroscopic Observation of a Hydrogenated Co Dimer Intermediate During Co Reduction on Cu(100) Electrodes. *Angew. Chem., Int. Ed.* **2017**, *56*, 3621−3624.

DOI: 10.1021/acs.jpcc.8b05634
J. Phys. Chem. C 2018, 122, 24658−24664